Available online at www.sciencedirect.com
SCIENCE DIRECT®
Journal of Nuclear Materials 337–339 (2005) 697–701
journal of nuclear materials
www.elsevier.com/locate/jnucmat

Interaction of ELMs and fast particles with in-vessel components in ASDEX Upgrade

A. Herrmann *, J. Neuhauser, V. Rohde, R. Dux, T. Eich, C.J. Fuchs, M.Y. Ye, ASDEX Upgrade team

Max-Planck-Institut für Plasmaphysik, EURATOM-IPP Association, Boltzmannstr. 2, D-85748 Garching, Germany

Abstract

Heat deposition onto plasma facing components outside the divertor by ELMs and fast particles has been investigated in ASDEX Upgrade. Heat fluxes up to tens of megawatts per square meter are found during ELMs on limiters and a few megawatts per square meter in between. The total deposited power on non-divertor structures can be up to 10% of the heating power and has to be considered for high power next step experiments. The mechanisms behind the observed heat load patterns are qualitatively understood. The main contributions come from fast ions created by neutral beam injection (and ion cyclotron minority) heating, and from ELMy energy bursts from the plasma edge.

PACS: 52.40.H; 52.55.Fa
Keywords: Power deposition first wall; Divertor; ASDEX Upgrade

1. Introduction

Divertor tokamaks, such as ASDEX Upgrade, are designed to receive the energy crossing the last closed flux surface (the separatrix) at specially designed targets, capable of handling tens of Megawatts per square meter. The power and energy handling capability of the divertor has been investigated thoroughly during the past few years and energy balances established from the heating power, the plasma radiation and the heat load to the divertor targets account for 100 ± 20% in ASDEX Upgrade [1]. There is strong evidence, that the scatter found in the power balance is not simply due to measurement errors, but due to variable heat deposition outside the divertor. CCD imaging of the inner vessel shows for certain discharge conditions hot spots at different locations. Thermographic investigation of ELM energy losses at ASDEX Upgrade and JET revealed that the energy detected in the divertor accounts for only about 50% of the midplane losses [2]. Parts of the outboard limiters and under special discharge conditions also in-vessel components far away from the plasma are heated up to aftershot equilibration temperatures of 400 °C as measured with thermocouples.

Although the heated parts outside the divertor contribute less than 10% to the overall energy balance, the local heat load results in surface temperatures up to the sublimation temperature of carbon and causes a significant erosion of material. In addition, components (e.g. water pipes) might be damaged due to local

* Corresponding author. Tel.: +49 89 3299 1388; fax: +49 89 3299 2580.
E-mail address: albrecht.herrmann@ipp.mpg.de (A. Herrmann).

0022-3115/$ - see front matter © 2004 Elsevier B.V. All rights reserved.
doi:10.1016/j.jnucmat.2004.10.126

overheating. The energy deposition to in-vessel components is investigated quantitatively by ELM-resolved thermography, and thermocouple measurements as well as qualitatively by CCD imaging.

The observed heat load patterns are caused by different loss mechanisms which will be discussed in the paper. Section 2 summarizes the experimental conditions. Section 3 discusses first orbit losses due to beam ionisation in the limiter shadow or the plasma edge. In Section 4 we discuss fast ion losses from the plasma core and the resulting fast ion population in the scrape-off layer (SOL), including related charge exchange effects. The effect of ELMs on the non-divertor heat load is presented in Section 5. The paper is briefly summarized in Section 6.

2. Experimental arrangements and vessel geometry

An overview of available diagnostics, their location at ASDEX Upgrade and a more detailed description of the infrared (ir) camera features are given in [3]. 12 limiters, 8 ICRH limiters and 4 protection limiters, are installed in ASDEX Upgrade. The protection limiters are geometrically about 1 cm behind the ICRH limiters ($R = 2.20$ m). Therefore they are efficiently shadowed for equilibrium configurations well adapted to the ICRH limiter shape (Fig. 1(a)), but are at least partly accessible along field lines for plasma shapes deviating strongly from it as shown in Fig. 1(b). In this figure, the protection limiter is kept at the geometric coordinates and the ICRH limiter 110° downstream in counter current direction is mapped along field lines onto the toroidal position of the protection limiter, which is in view of the ir-camera.

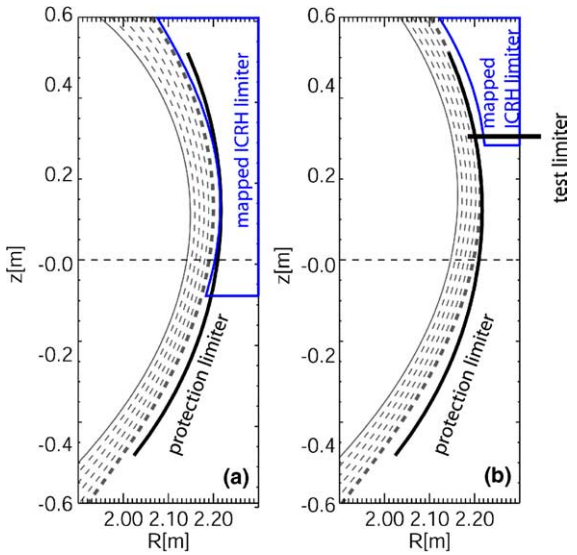

Fig. 1. Magnetic limiter configurations. The protection limiter is shown at its geometric position. The ICRH limiter 110° downstream in counter current direction is mapped along field lines onto the geometric position of the protection limiter. (a) The magnetic flux surfaces are parallel to the limiter contour and the protection limiter is shadowed by the ICRH limiter. (b) The whole protection limiter is in front of the ICRH limiter.

This partial shadowing is important for the interpretation of the limiter load measurements reported below, especially with respect to fast ion heat load from the different neutral beam injection geometries available on ASDEX Upgrade. Details of the NBI system can be found in [4,5].

3. First orbit losses from neutral beam injection

CCD imaging and ir-cameras show for certain discharge conditions heat deposition on parts of some outboard ICRH and protection limiters which are toroidally localized. This deposition can be attributed to first orbit losses from the adjacent neutral beam injector box, i.e. to ions created in the limiter shadow or edge plasma in front of this box directly hitting wall elements on their first turn. These high energy ionized particles essentially follow field lines and dissipate their energy immediately at the intersection of the field line with the nearest in-vessel component. The amount of edge ionized neutrals depends on the ionisation probability, which in turn depends on the energy of the beam and the density profile in front of the beam port.

Accordingly, a limiter close to one injector box gets hot, if this box is active, but is essentially unaffected by first orbit losses from the box 180° away as shown in Fig. 2 for a 5 MW type-I ELMy H-mode discharge. The heating of the active ICRH limiter is caused by transport losses from the core plasma and is not significantly effected by the change of the NBI geometry (Fig. 2(d)). Apart from the first orbit losses no significant heat load is found at the protection limiter, as expected from the magnetic geometry (Fig. 1(a)), which shows the protection limiter in the shadow of the ICRH limiter.

4. Power load by core fast ion losses

In addition to the first orbit losses described in the previous section, fast ions created by neutral beam injection or ion cyclotron minority heating in the core plasma can be transported to the edge before slowing down. These ions are expected to deposit their energy onto limiters in a toroidally more symmetric fashion. Still, the amount of fast ions showing up in the SOL can depend significantly on the neutral beam injection geometry,

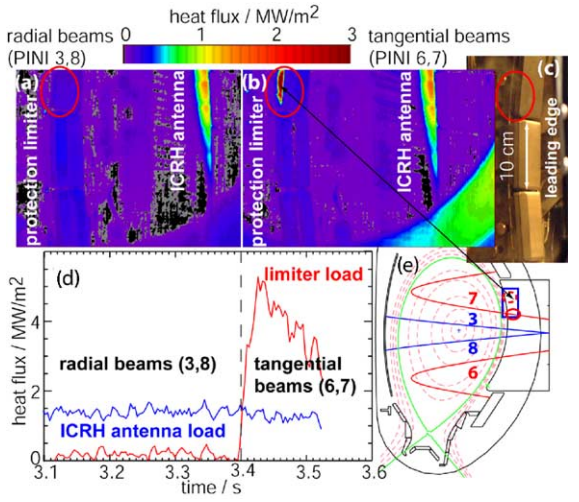

Fig. 2. Ir-view into the AUG vessel during operation with radial (a) and tangential beams (b). (c) Visible view to the protection limiter. The circle indicates the position of the hot spot. (d) Time traces of the heat flux to the protection and the ICRH limiter, respectively. (e) Beam geometry. Source 7 in magnetic view to the limiter causes a hot spot due to first orbit losses.

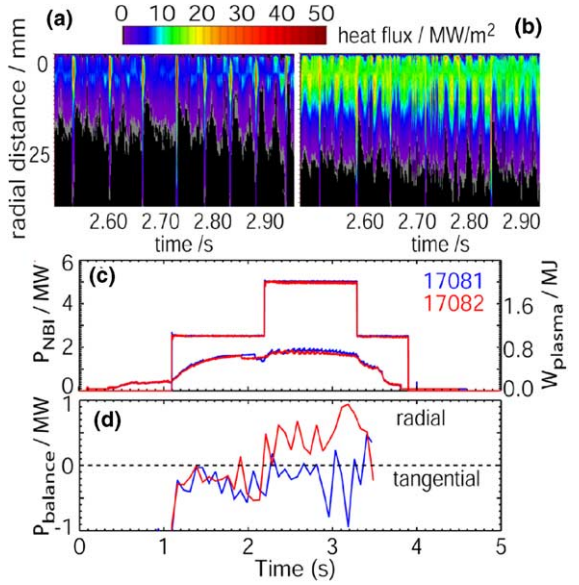

Fig. 3. Perpendicular heat load to the test limiter for comparable discharges with (a) tangential and (b) radial beam heating in dependence on the radial distance to the leading edge. (c) NBI heating power and plasma energy for both discharges. (d) The power balance (P_{in}–P_{rad}–P_{div}) is unbalanced if the test limiter receives more energy.

which determines how many ions are created on passing and banana trapped orbits, respectively.

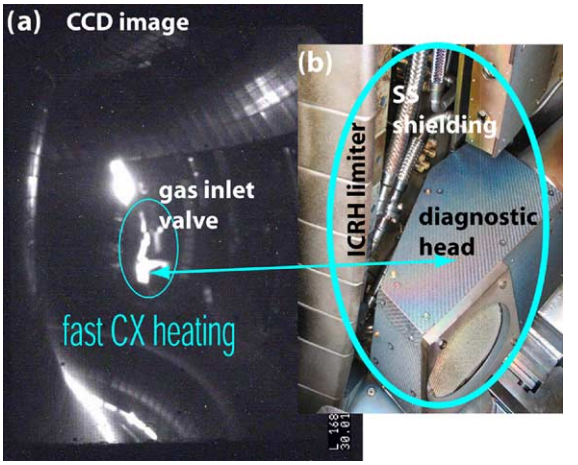

Fig. 4. (a) View into the ASDEX Upgrade vessel during a discharge. (b) Picture of the installation in the shadow of an ICRH limiter. Charge exchange neutrals from fast banana trapped ions in regions with high neutral density near to the gas inlet heats up diagnostic heads and stainless steal shielding deep (10 cm) in the shadow of the ICRH protection limiter.

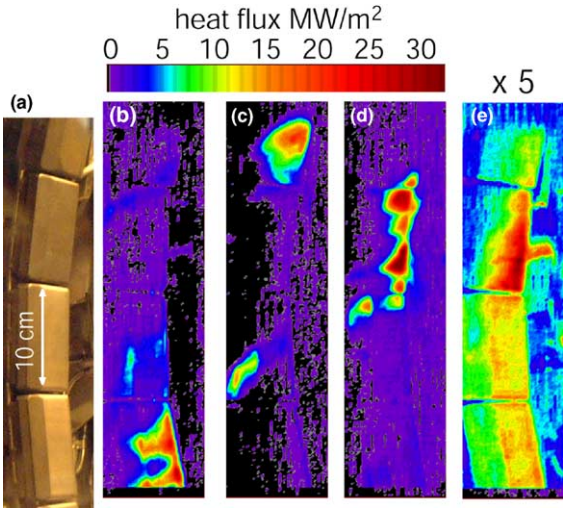

Fig. 5. (a) Picture of the protection limiter shown in the ir-view. ((b)–(d)) Heat load pattern at the protection limiter for different ELMs (e) The ELM averaged (37 ELMs) heat load is below 5 MW/m^2. The structure was measured with 50 μs snapshot time and 500 μs frame rate.

To measure the fast ion population profile in the SOL, a test limiter was exposed at the midplane manipulator positioned about 30 cm above the horizontal midplane. The limiter was made of CFC as presented in [6] but without the tungsten layer and was exposed to the SOL plasma at a position 5 mm radially in front of the ICRH limiter but magnetically about 30 mm out of the limiter shadow (Fig. 1(b)). For the measurements

reported here, the limiter was exposed during two type-I ELMy H-mode shots with 5 MW heating power injected by tangential beams located near to the test limiter, and more radial beams toroidally 180° away, respectively. The heat load to the tip of the limiter which is about half the parallel heat flux along field lines changes from about 5 MW/m^2 for the tangential beams to 12 MW/m^2 for the radial beams as shown in Fig. 3(a) and (b).

The power balance, taking into account the radiation losses and the power deposition to the lower divertor, is unbalanced by about 500 kW or 10% of the heating power for the shot with higher test limiter load (Fig. 3). This is about the heat load deposited in the gap between the end of the outer divertor and the test limiter, which is not included in the power balance. For both shots, the ELM heat load is nearly independent of the neutral beam injection geometry.

The reason for the measured difference in the heat load to the test limiter is the neutral beam injection geometry. Particles injected more radial in the plasma have a reduced parallel velocity component and as a consequence, a higher fraction is trapped on banana orbits at the low field side of the plasma. The critical pitch angle, below which the particles are trapped on banana orbits, is $\tan(v_\parallel/v_\perp) < 43°$ in ASDEX Upgrade. The pitch angle is about 70° for the tangential and about 20° for the radial beam at the deposition maximum. The particles on banana orbits with a width of a few cm can penetrate deep into the SOL and heat the test limiter. In addition, ripple trapped banana particles exist at energies comparable to the pedestal temperature with banana stagnation points in the SOL. A quantitative estimation of the fraction of banana transported power into the SOL needs kinetic code calculations taking into account the magnetic field ripple and is in preparation.

The same test-limiter was used for heat flux decay measurements in the far SOL region by changing the distance between the limiter and the separatrix from 3 to 7 cm. The heat load to the limiter tip is reduced from 16 to 6 MW/m^2. The resulting e-folding length for the heat flux in the far SOL region is about 4 cm. The heat flux e-folding length across the radial limiter surface, as measured for different limiter to separatrix distances, is nearly constant at about 8 mm, as expected in a limiter shadow with fixed connection length.

The large e-folding length of a few centimeters in a region far from the separatrix, but outside the limiters is in correspondence to the long tail of heat flux profiles as measured in the lower divertor which seems to be nearly constant over the observed distance of about 2 cm mapped to the midplane. High temporal resolution measurements of temperature and density in the edge also show a long tail in between and during ELMs [7,8].

In addition to direct limiter deposition, fast ions can undergo charge exchange with edge neutrals, especially in the case of increased local neutral density, e.g. in front of a local gas puff valve. This can cause heat fluxes up to 1 MW/m^2. An example is shown in Fig. 4. Parts of a diagnostic deep (5 cm) inside the ICRH limiter shadow and the stainless steel shielding of a water cooling pipe were damaged due to a pronounced production of energetic CX particles near to the gas valve in this section.

Since the CX cross section significantly drops with increasing ion energy, partially slowed down ions in the 10 keV region are preferentially removed by CX, while high energy ions may survive and finally hit the limiters as described above. An obvious way to minimize this localized effect is to replace the low field side gas puff by the toroidally distributed divertor gas puff available in ASDEX Upgrade.

5. ELM heat load outside the divertor

As shown in the previous sections, the heat load to non divertor components can be caused by the interaction of neutral beams with the core plasma or with edge neutrals. The resulting parallel heat load is small or even comparable to the contribution of ELMs to the non divertor heat load (see Fig. 5). This section summarizes a few measurements on ELM heat load to a protection limiter of ASDEX Upgrade. This limiter is not loaded, even during ELMs, if it is magnetically shadowed by the adjacent ICRH limiter as seen in Figs. 1 and 2. The limiter was active for the measurements discussed below. The extrapolation from the local measurement to a toroidally averaged load is done by using additional information from thermocouple measurements and cooling water calorimetry as described in detail in [3]. In this paper we concentrate on the ELM related heat flux pattern to the limiter. An ELM power balance using the newly developed method for radiation evaluation [9] is the topic of a future paper. As reported from ir measurements of the heat load pattern in the upper divertor [10], the ELM heat deposition shows a structure remote from the strike point which can be described by radially extended heat sources at n toroidal locations in the outer midplane mapped along field lines to the divertor. This ELM structure is smoothed out near the separatrix due to the x-point shear so that the heat flux to the strike point in the divertor is toroidally symmetric. The protection limiter remote from the separatrix should receive these structured heat loads also. Examples from different ELMs in one type-I ELMy H-mode discharge are shown in Fig. 5. The height of one limiter tile is 10 cm and corresponds to about 50 cm projected toroidally along the 10 m circumference in ASDEX Upgrade for a safety factor q_{95} of 4.

The examples of Fig. 5 show the variation of the observed structure in periodicity and local concentration. The absolute values of the perpendicular heat flux is similar for all hot stripes between 20 and 30 MW/m^2. The

stripes are deposited simultaneously or their deposition time is much shorter than the 50 μs snapshot time of the measurement. The high heat fluxes in the tens of MW/m^2 range are consistent with ELM heat flux profiles measured in the lower divertor. These profiles show a wide tail with an e-folding length in the cm range which would result in a limiter heat flux comparable to that at the outermost divertor edge, as shown in [3]. The energy content of a single stripe as estimated from the wetted area at the protection limiter, the measured heat flux and a deposition time of 50 μs is about 2 J which has to be compared to 20 kJ plasma energy loss per ELM. Here, the integration time of the ir-camera is used as the energy deposition time. The true ELM deposition time might be longer. The upper limit is given by the frame rate of 500 μs/frame, because the stripes are never observed in consecutive frames. The ELM averaged heat flux is more than a factor of 5 lower, as expected from the stochastic behaviour of the ELMs (Fig. 5(e)).

6. Summary

The appearance of hot spots with heat fluxes of a few MW/m^2 at in-vessel components has been analysed in ASDEX Upgrade and the dominant mechanisms involved are qualitatively understood. The main contributions come from fast ions created by neutral beam injection (and ion cyclotron minority) heating, and from ELMy energy bursts from the plasma edge.

The ELM heat flux to in-vessel components is high and can reach tens of MW/m^2 at the active ASDEX Upgrade limiters. Nevertheless, the energy deposition of a single stripe is only in the order of a few joule, i.e. a small fraction of the ELM mid-plane loss The averaged heat flux to the limiter is more than a factor of 5 less, due to the stochastic behaviour of the ELMs. No ELM heat load is measured, if the protection limiter is in the magnetic shadow of the ICRH limiter.

While the physical origin is difficult to avoid, the consequences might be mitigated in the future by a smoother first wall design especially at the magnetic low field side, distributing the fast particle and ELM heat load onto a larger wetted area.

References

[1] J.C. Fuchs, D. Coster, A. Herrmann, et al., J. Nucl. Mater. 290–293 (2001) 525.
[2] A. Herrmann, T. Eich, S. Jachmich, et al., J. Nucl. Mater. 313–316 (2003) 759.
[3] A. Herrmann, T. Eich, V. Rohde, et al., Plasma Phys. Control. Fus. 46 (2004) 971.
[4] A. Stabler, J. Hobirk, F. Leuterer, et al., Fus. Sci. Technol. 44 (2003) 730.
[5] B. Streibl, P.T. Lang, F. Leuterer, et al., Fus. Sci. Technol. 44 (2003) 578.
[6] M.Y. Ye, H. Maier, H. Bolt et al., J. Nucl. Mater., these Proceedings. doi:10.1016/j.jnucmat.2004.10.163.
[7] J. Neuhauser, H.S. Bosch, D. Coster, et al., Fus. Sci. Technol. 44 (2003) 659.
[8] J. Neuhauser, D. Coster, H.U. Fahrbach, et al., Plasma Phys. Control. Fus. 44 (2002) 855.
[9] J.C. Fuchs, T. Eich, A. Herrmann, et al., J. Nucl. Mater., these Proceedings. doi:10.1016/j.jnucmat.2004.09.054.
[10] T. Eich, A. Herrmann, J. Neuhauser, et al., Phys. Rev. Lett. 91 (2003).